Neuroscience Research 93 (2015) 116–127

Contents lists available at ScienceDirect

Neuroscience Research

journal homepage: www.elsevier.com/locate/neures

Review article

Current models of the marmoset brain

Tsutomu Hashikawa, Reiko Nakatomi, Atsushi Iriki*

Laboratory for Symbolic Cognitive Development, RIKEN Brain Science Institute, Wako, Saitama 351-0198, Japan

ARTICLE INFO

Article history:
Received 6 November 2014
Received in revised form 7 January 2015
Accepted 13 January 2015
Available online 26 March 2015

Keywords:
Common marmoset
Cytoarchitecture
Stereotaxic atlas
Brain models
Volume rendering
MRI

ABSTRACT

Since the availability of the common marmoset monkey as a primate model in neuroscience research has recently increased, much effort has been made to develop a reliable guide of the brain structures of this species. In this article, we review the development of the marmoset brain atlas and discuss a newly developed brain model, which was reconstructed from histological sections under volume-rendering technology. This kind of brain model allows virtual sections to be constructed on any axis, with nomenclatural annotations to structures in situ. This model is also applicable for the identification of structures revealed in magnetic resonance imaging studies. The brain model is accessible at the following web address: http://brainatlas.brain.riken.jp/marmoset/modules/xoonips/listitem.php?index_id=66.

Contents

1. Introduction

As an animal model of non-human primates, the common marmoset (*Callithrix jacchus*), a New World monkey, has been used in a variety of biomedical studies that have ranged in topic from reproductive medicine to social behavioral science (Heig, 1999; Norscia and Palagi, 2011; Ash and Buchanan-Smith, 2014). The inevitable evolution of gene manipulation technologies means that the use of the common marmoset in these research fields will increase (Sasaki et al., 2005), Moreover, since genome of this species has been recently sequenced, it is anticipated that there will be rapid surge in the interest of primate biology (Marmoset Genome Sequencing and Analysis Consortium and Marmoset Genome Sequencing and Analysis Consortium, 2014).

Along with biological sciences, the marmoset can be a useful animal model in neuroscience research (Kishi et al., 2014). This is because among the primates, the common marmoset (1) is available at a relatively low price with mature adults being small in size (300 g or so) (Power et al., 2001). Thus, it is easier to house and handle these monkeys in a laboratory setting; (2) shows high fertility (giving birth to non-identical twins twice/year) and earlier sexual maturity (~15 months) (Stevenson, 1976; Mano et al., 1987). This means that certain genetic aspects of neural functions can be analyzed (Sasaki et al., 2014), which is important given that most genetic studies that have taken place so far have been conducted in mice; and (3) has a structurally well-developed brain sharing similar characteristics across various primate species (Paxinos et al., 2012). Common features of brain structures in primates make

* Corresponding author. Tel.: +81 48 467 9637.
E-mail address: iriki@brain.riken.jp (A. Iriki).

http://dx.doi.org/10.1016/j.neures.2015.01.009

rather direct comparisons possible among the species, and the comparative approach seems especially important in marmoset studies. Since relatively limited information is available regarding the common marmoset itself, data collected on other primates have been helpful when considering correlations between structure and function in the marmoset brain. Thus, a combination of knowledge of research on Old World primates and new insights from genetic approaches in marmosets will provide a better, more comprehensive understanding of brain functions.

Brain atlases are useful in identifying and analyzing neurological structures. At present, several atlases are available for the common marmoset (Palazzi and Bordier, 2008; Yuasa et al., 2010; Tokuno et al., 2009; Paxinos et al., 2012). Brain structures in these atlases are delineated cytoarchitectonically in Nissl sections, and/or chemoarchitectonically in immunohistochemical (e.g. for calcium binding proteins) or histochemical (e.g. for acetylcholinesterase) sections.

In addition to histological analyses, magnetic resonance imaging (MRI) technology that has become a routine means to specify functional areas in the brain, requires interactive structural information for image acquisition. Since brain atlases are not necessarily sufficient for such analyses, an additional model of the common marmoset brain has been proposed, in order to fit in with current research demands. Given the above background, we developed a web-accessible brain model of the common marmoset monkey, and compared features of this model to that of previously reported brain atlases for this animal species.

2. Methodological consideration

2.1. Architectural bases of the brain atlas

Fundamentally, brain structures are cytoarchitectonically identified based on their appearance and type of neuronal staining, i.e., Nissl staining. Major criteria that have been used to specify brain regions or structures include staining density, cell body size, pattern of accumulation and/or distribution, and locations of cell aggregates with relation to their neighbors. The interpretation of staining patterns, however, is not simple or straightforward, and can thus be analyzed differently among individuals. Descriptions in cat brain atlases (Berman, 1968; Berman and Jones, 1982), for example, should be appreciated and referred to when never a new brain atlas is being developed. This is, because descriptions in these atlases are considerably detailed in terms of cytoarchitectonic features of brain structures that commonly appear across species. In primates, however, thorough, comparative studies should be carried out since they have characteristic brain regions that are different from or absent in rodents and carnivores, e.g., the well-developed neocortex/striatum of the cerebrum and the pulvinar of the thalamus.

In producing brain atlases, cytoarchitectonic characterizations by Nissl staining can be supplemented by myeloarchitectonic features with dense staining of fiber bundles and tracts. For example, the primary auditory cortex and area TE of the temporal lobe are characterized by dense myelin staining in the middle layers of the cortex.

In addition to the characterization of brain structures by cyto- and myelo-architectural methods, chemoarchitectural characterization is also necessary for the delineation of several brain structures. One example of such an approach includes histochemical staining for acetylcholinesterase and immunohistochemical staining for calcium binding proteins (parvalubumin, calbindin), tyrosine hydroxylase, neurofilament protein etc. Recently, techniques in molecular biology have also been employed to aid in the visualization of particular brain regions or neural cells (Carson et al., 2005; Hevner, 2007; Jessberger and Gage, 2007; Lein et al., 2007; Molyneaux et al., 2007; Ng et al., 2009). Thus more detailed atlases that incorporate interdisciplinary aspects are necessary not only in rodents, but also in the common marmoset.

2.2. Stereotaxic coordination

Most of the previously published brain atlases have been produced with stereotaxic coordinates. This is the case for the common marmoset as well. In the atlas, three axial (coronal, horizontal and sagittal) planes have been utilized to localize brain structures in 3-demensional (3D) space. The sagittal zero plane is the plane through the midline of the left and right hemispheres. Horizontal zero plane, however, is not as clearly delineated and varies among the atlases, depending on the axial line settings. The horizontal axial plane can be set on either the line passing through the center of the opening of the external acoustic meatus and infraorbital margin of the maxilla (i.e., orbitomeatal line) as adopted in most animals; 10 mm above the orbitomeatal line, known as the Horsley-Clarke zero plane (e.g., Berman, 1968; Berman and Jones, 1982); the line passing through the center of the opening of the external acoustic meatus and maxillary incisor; or the line passing through the center of the anterior and posterior commissure (Martin and Bowden, 1996). The former three positions have been adopted for neurosurgical use, while the latter coordinates are mostly applied in radiological studies. The coronal zero plane typically lies on the interaural line which passes through the center of the external acoustic meatus on both sides, and sometimes in the center of the anterior commissure (Martin and Bowden, 1996). However, since the horizontal axial plane can be variably set, coronal planes also tend to vary depending on the adopted horizontal axis. This is because coronal planes form right angles against horizontal planes at all times. Thus, methodological information of all atlases should be consulted in order to determine how horizontal/coronal planes are constructed.

Among the stereotaxic planes, the coronal planes have been described most intensively, while horizontal and sagittal planes have only been superficially described. Such biased descriptions result in difficulties when investigators attempt to understand brain structures in 3D. However, conception of the steric aspect is no less important, especially for spatially complicated brain structures. To supplement the difficulties in 3D reconstruction, efforts have been made in rodents by employing computer-assisted technology, using data from MRI, Nissl and/or gene expression analyses (Ma et al., 2005; Hjornevik et al., 2007; Dorr et al., 2008; Hawrylycz et al., 2011; Kumazawa-Manita et al., 2013). Although the conversion of histological information to MRI volume data (Saleem and Logothetis, 2012), no comparable studies are available in the common marmoset. Digital brain atlases organized with stereotaxic coordinates for the common marmoset have been recently made accessible over the web (Tokuno et al., 2009; Paxinos et al., 2012). The discussion of the evolution of brain atlas construction reveals the progression of data acquisition technology. Along with current research demands, the advancement in technology encourages the development of modern brain models. Thus, a new version of the marmoset brain atlas will be introduced later in this article. The new atlas is based on a volume-rendered brain model with axial-free coordinates, i.e., the model is ready for any coordination including stereotaxic axes, showing virtual brain structures delineated by their histological features (see below).

3. Stereotaxic coordination and spatial localization

Thus far, all of the brain atlases that have been published on the common marmoset have been described using stereotaxic coordinates (Palazzi and Bordier, 2008; Hardman and Ashwell, 2012; Paxinos et al., 2012). While such atlases are useful for localizing

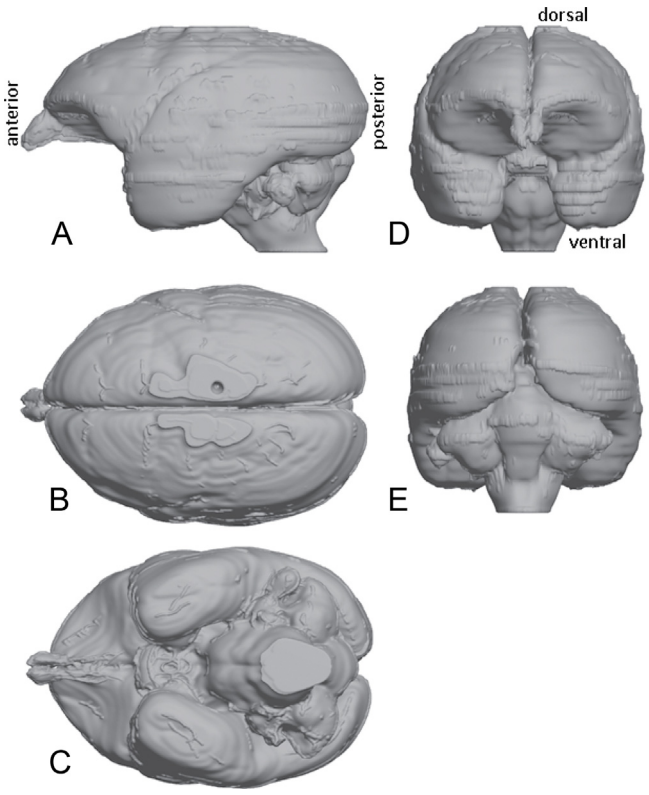

Fig. 1. Surface view of a marmoset brain model, reconstructed from Nissl stained histological sections. Horizontal sections with 200-μm intervals were used for the reconstruction. (A) Left lateral view, (B) dorsal view, (C) ventral view, (D) frontal view, (E) caudal view.

architectonically identified structures in sectional plates with numerical coordinates, the localization of structures in 3D space is difficult. This is, because direct information for the spatial continuation of every brain structure is hard to obtain from such atlases. Moreover, information on the continuation of structures is substantially important for 3D reconstruction.

A recent increase of MRI experiments in the common marmoset (Hikishima et al., 2011, 2013; Sawada et al., 2014) has prompted the development of a new brain atlas – one that coordinates of more detailed structural information so that it can be used with volume-rendered MRI data. MRI studies can provide spatial

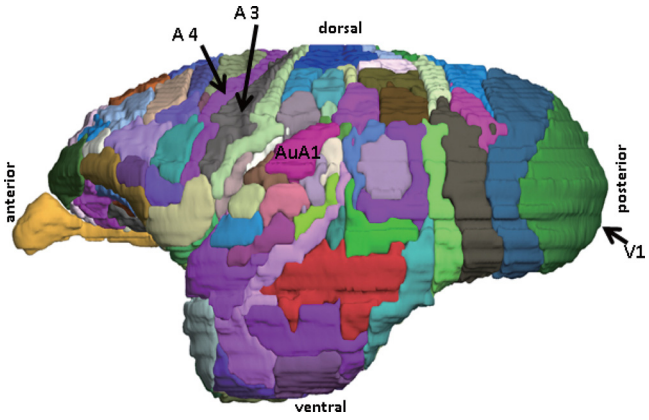

Fig. 2. Surface view of the left cerebral cortex. Delineated cortical regions are depicted by the same colors as shown in Table 1. In the model, every colored structure can be specified by an annotation, e.g., green for the primary visual cortex (V1), reddish pink for the primary auditory cortex (AuA1), darkly pink for the primary motor cortex (A4), brown for the somatosensory cortex area 3 (A3), etc.

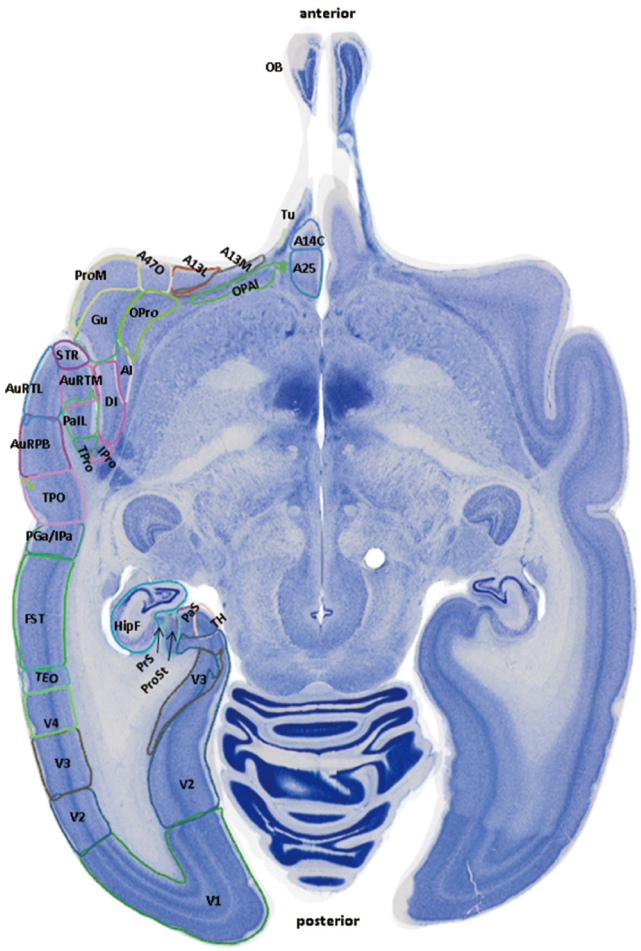

Fig. 3. An example of a horizontal section with delineated cortical regions, in which information for the cortical delineation in coronal sections (Paxinos et al., 2012) was converted using SG-eye software. A colored line drawing for each cortical region (see the list in Table 1) overlaps the Nissl image. Abbreviations: AI, agranular insular cortex; A13L, area 13, lateral part; A13M, area 13, medial part; A14C, area 14, caudal part; A25, area 25; A47O, area 47, orbital part; AuRPB, auditory cortex, rostral parabelt; AuRTL, auditory cortex, rostrotemporal lateral area; AuRTM, auditory cortex, rostrotemporal medial area; DI, disgranular insular cortex; FST, fundus of the superior temporal sulcus area of cortex; Gu, gustatory cortex; HipF, hippocampal formation; IPro, insular proisocortex; OB, olfactory bulb; OPAl, orbital periallocorte; OPro, orbital proisocortex; PaIL, parainsular cortex, lateral part; PaS, parasubiculum; PGa/IPa, parietal areas PGa and IPa; ProM, proisocortical motor region; ProSt, prostriate area; PrS, presubiculum; STR, superior temporal rostral area; TEO, temporal area TE, occipital part; TPO, temporo-parieto-occipital association area; TPro, temporal proisocortex; TH, temporal area TH; Tu, olfactory tubercle; V1, visual area 1; V2, visual area 2; V3, visual area 3; V4, visual area 4.

information on the location of brain regions of interests even in living animals. However, spatial resolution is rather poor in MRI studies; thus, complementary structural information needs to be collected from appropriate brain atlases.

4. Volume-rendered 3D images: a combination of histological staining and MRI technologies

Being motivated by recently developed digital atlases of common marmoset brains, which include cytoarchitectonic and chemoarchitectonic details with stereotaxic information (Tokuno et al., 2009; Paxinos et al., 2012), an attempt was recently made to combine these methods on sectional planes of the same brain (Newman et al., 2009). In 2009, Newman et al. successfully published a histological and magnetic resonance (MR)-based atlas describing structures in coronal sections, in which relative rostrocaudal levels were converted to their sectional plates from the

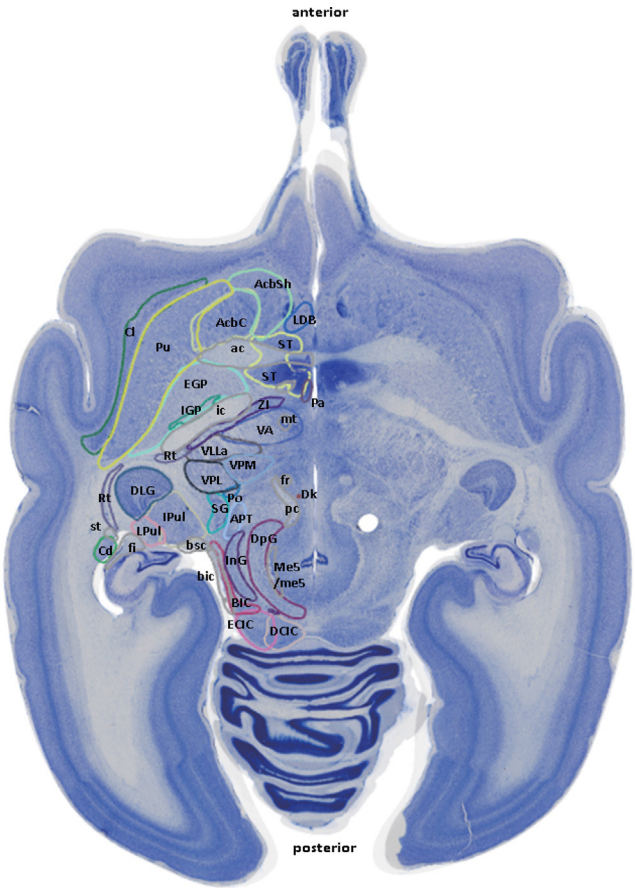

Fig. 4. An example of a horizontal section with delineated inner brain structures, in which information for the delineation in coronal sections (Paxinos et al., 2012) was converted using SG-eye software. A colored line drawing for each inner structure overlaps the Nissl image. Abbreviations: ac, anterior commissure; AcbC, accumbens nucleus, core; AcbSh, accumbens nucleus, shell; APT, anterior pretectal nucleus; BIC, nucleus of the brachium of the inferior colliculus; bic, brachium of the inferior colliculus; bsc, brachium of the superior colliculus; Cd, caudate nucleus; Cl, claustrum; DCIC, dorsal cortex of the inferior colliculus; Dk, nucleus of Darkschewitsch; DLG, dorsal lateral geniculate nucleus; DpG, deep gray layer of the superior colliculus; ECIC, external cortex of the inferior colliculus; EGP, external globus pallidus; fi, fimbria of the hippocampus; fr, fasciculus retroflexus; ic, internal capsule; IGP, internal globus pallidus, InG, intermediate gray layer of the superior colliculus; LDB, lateral nucleus of the diagonal band; IPul, inferior pulvinar; LPul, lateral pulvinar; Me5/me5, mesencephalic trigeminal nucleus and tract; mt, mammillothalamic tract; Pa, paraventricular hypothalamic nucleus; pc, posterior commissure; Po, posterior thalamic nuclear group; Pu, putamen; Rt, reticular nucleus; SG, suprageniculate thalamic nucleus; ST, bed nucleus of the stria terminalis; st, stria terminalis; VA, ventral anterior thalamic nucleus; VLLa, ventral lateral thalamic nucleus, lateral part; VPL, ventral posterolateral thalamic nucleus; VPM, ventral posteromedial thalamic nucleus; ZI, zona incerta.

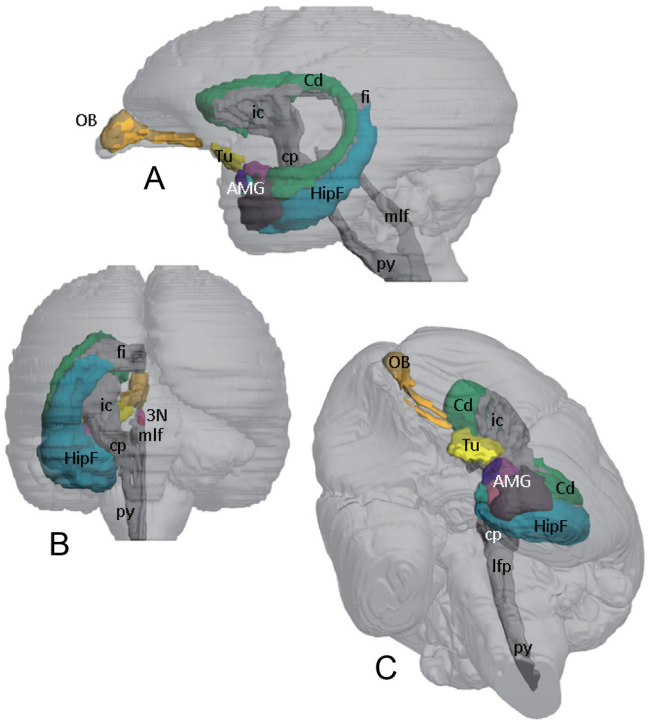

Fig. 5. Lateral (A), caudal (B), and ventrolateral (C) views of example structures in a translucent brain space. Abbreviations: AMG, amygdala; Cd, caudate nucleus; cp, cerebral peduncle; fi, fimbria of the hippocampus; HipF, hippocampal formation; ic, internal capsule; lfp, longitudinal fasciculus of the pons; mlf, medial longitudinal fasciculus; OB, olfactory bulb; py, pyramidal tract; Tu, olfactory tubercle; 3N, oculomotor nucleus.

atlas by Stephan et al. (2009). The combination of histology and MRI technology seems to make sense in doing experimental studies since functional aspects of brain structures can be revealed by in vivo MRI studies, while their precise structural interpretation can be achieved by histological examinations. The invaluable aspect of MRI data is that it is volume-rendered, and can be used for axially flexible 3D reconstruction of brain models. Ideally, it should be possible to localize brain structures in such a model with no consideration of ordinal stereotaxic coordination. Such a brain model, however, obviously needs histological data for every brain structure with information rendered in the brain volume. Thus, in the current review we proposed a web-accessible and volume-rendered brain model with histological information for the common marmoset (http://brainatlas.brain.riken.jp/marmoset/modules/xoonips/listitem.php?index_id=66). This brain model was developed in the Laboratory for Symbolic Cognitive Development in Brain Science Institute at RIKEN (RIKEN BSI), Japan. The following is an introduction of the axial-free common marmoset brain model, which is applicable for any brain axis including ordinal ones used in stereotaxic coordinates. For further details, please refer to the products section of the above URL.

5. Axial-free 3D brain model

For production of an axial-free steric brain atlas, a brain from the common marmoset monkey (*Callithrix jacchus*; female; 2.3 years old; weighing 310 g) was obtained from the Central Institute for Experimental Animals (CIEA), Kawasaki, Japan. Prior to histological preparation, MRI was performed on this animal (Hikishima et al., 2011). After perfusion, the skull with the animal's brain was placed onto a stereotaxic apparatus, in which the horizontal axis was set on the orbitomeatal line and reference marks were made on the right side with carbon shafts (0.5 mm in diameter). The horizontal axis, passed through the coronal plane 3.5 mm rostral to the interaural line and horizontal zero plane, 2.0 mm and 2.5 mm lateral to the midline, respectively. The brain was embedded in gelatin and 50-μm-thick frozen sections were cut horizontally, mounted on glass slides, and stained with thionine. Photomicrographs were taken from the sections with a virtual slide scanner VS-100 (Olympus, Tokyo, Japan), and the imaged data were processed using Photoshop (Adobe, CA, USA). DATA was then imported into SG-eye software (Fiatlux, Tokyo, Japan). Using this software that we developed for these types of studies (Kumazawa-Manita et al., 2013) and the data obtained from horizontally-cut histological sections we constructed a 3D digital volume-rendered marmoset brain model. Structures described in the marmoset brain atlas (Paxinos et al., 2012) are listed in Table 1, and are organized hierarchically. With

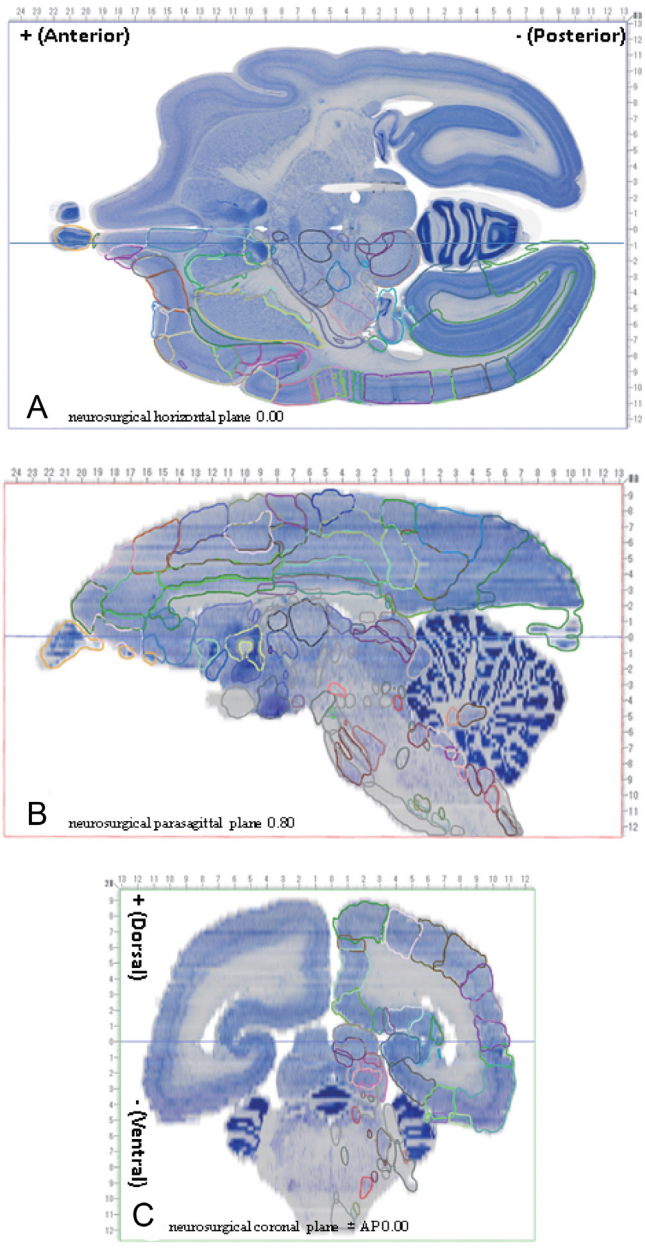

Fig. 6. Virtual images reproduced from the model: horizontal zero plane (A), parasagittal plane 0.8 mm lateral from midline (B), and coronal zero plane in neurosurgical stereotaxic coordinates. Lines in each image indicate approximate parasagittal (A) and horizontal (B and C) levels for the sectioning. Plane levels anterior and dorsal from the coronal and horizontal zero axes, respectively, have positive values, and vice versa. Scale marks are shown in mm.

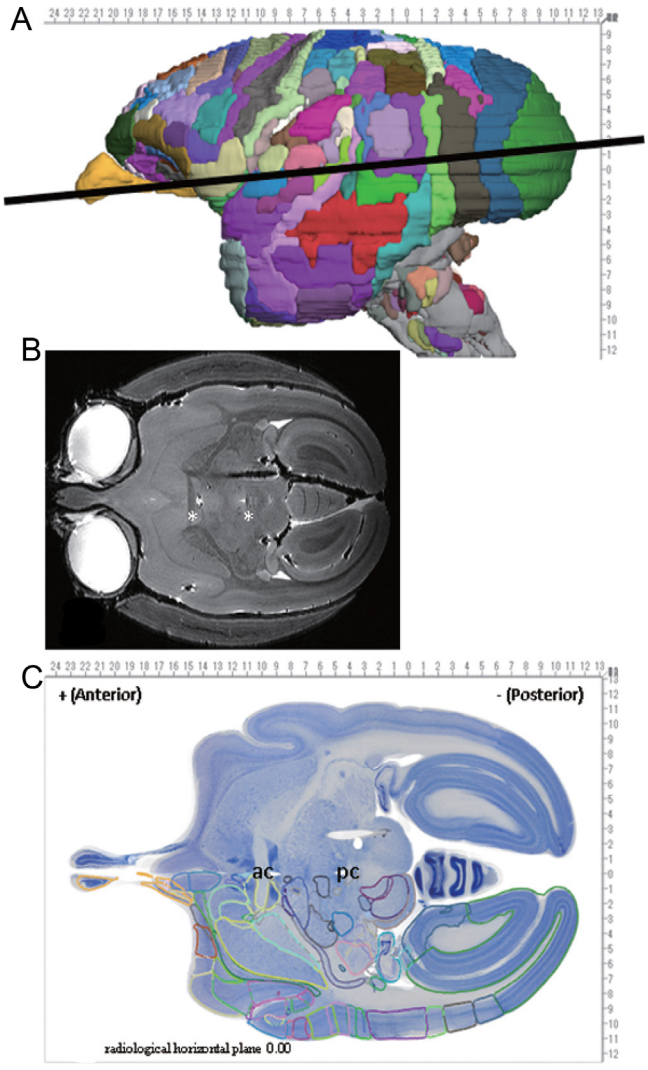

Fig. 7. An example of arbitrarily cut planes from the model. The line in A indicates the radiological axis, which passes through the center of the anterior and posterior commissures. A magnetic resonance image through this axis was obtained, as shown in B. Asterisks indicate the location of the anterior and posterior commissures. The brain model was reconstructed from this animal. C depicts a histological plane at approximately the same level as in A and B, which has annotations of delineated brain structures. Fig. 7B was referred from the brain atlas edited by Iriki et al. (in press).

the exception of tiny-delineated brain regions, most structures are presented by individual colors and reconstructed in 3D.

Fig. 1 shows a whole view of the current model of the marmoset brain reconstructed from the histological data. The model can be rotated and viewed from any directions, e.g., left-side view (Fig. 1A), dorsal view (Fig. 1B), ventral view (Fig. 1C), frontal view (Fig. 1D), and caudal view (Fig. 1E). On the surface of the cerebrum, cortical regions were localized with expedient color (Fig. 2), e.g., primary visual area (V1) with green color, primary auditory cortex (AuA1) with reddish pink, primary motor area (A4) with dark-pink, area 3 (A3) with brown, etc. These colors are compatible to those in Table 1. A previous atlas (Paxinos et al., 2012) was referred to for the delineation of cortical areas in this model. Information in Paxinos' atlas for cortical delineation in coronal sections was thoroughly converted to virtual coronal sections reconstructed from this volume-rendered model, in which sectional levels were adjusted manually. Horizontally-cut virtual sections were obtained from this model and information of cortical delineation was finally converted to actual horizontal sections. These were confirmed further by histological features of the regions, if necessary. Examples of cortical delineation after conversion are shown in the horizontal sections of Fig. 3. Although it may be appropriate to account for tissue shrinkage or distortion of histological sections, which would be especially important for construction of atlases in stereotaxic coordinates, these issues were not taken into serious consideration in the current model because, in order to cope with these issues, it should be sufficient to cross-reference histological sections to radiological MRI data from the same animal. In the model, therefore, the histological data manually adjusted to be compatible with slice images from MRI data; matching the size, sectional level, and location of particular brain structures that were adopted as representative sections, as demonstrated in this series of 2D images: http://brainatlas.brain.riken.jp/marmoset/modules/xoonips/listitem.php?index_id=66.

As for the inside view of the model, major structures, including nuclei and fiber tracts, were delineated and identified using similar methods that were used for the cortex. Representative horizontal sections from the model are shown in Fig. 4. A typical feature of a volume-rendered model is that reconstructed structures can be visualized continuously. Thus, a whole extension of the structures in 3D from any direction can be observed in Fig. 5.

Because of the axial-free nature, one of the key features of this model is that a section can be made from any plane. Neurosurgical horizontal (Fig. 6A), parasagittal (Fig. 6B), and coronal (Fig. 6C) plates are shown as examples in stereotaxic coordinates. The highest histological resolution could be obtained in horizontal planes, and this was expected because horizontal sections were used from the sectional database used to reconstruct the model. This is a characteristic feature of the present model, and contrasts with previously published marmoset atlases that mostly used coronal sections for the localization of brain structures. In addition to conventional stereotaxic planes, radiological

Table 1

Brain structures listed in the table are arranged in hierarchical order. Nomenclature and abbreviations were adopted from the marmoset brain atlas of Paxinos et al. (2012). Colors assigned for major structures in the list correspond to the colors for individual structures in the 3D model. Tiny structures depicted in black are not specifically localized in the model in order to avoid overcomplicating the model components.

WHOLE BRAIN	WHOLE
1. FOREBRAIN (TELENCEPHALON and DIENCEPHALON)	FORE
1.1. TELENCEPHALON	TEL
1.1.1. OLFACTORY BULB	OLB
Accessory olfactory bulb	AOB
Anterior olfactory nucleus	AON
Ependyma & subependymal layer	E
External plexiform layer of the accessory olfactory bulb	EPIA
External plexiform layer of the olfactory bulb	EPI
Glomerular layer of the accessory olfactory bulb	GlA
Glomerular layer of the olfactory bulb	Gl
Granule cell layer of the accessory olfactory bulb	GrA
Granule cell layer of the olfactory bulb	GrO
Internal plexiform layer of the olfactory bulb	IPl
Mitral cell layer of the accessory olfactory bulb	MiA
Mitral cell layer of the olfactory bulb	Mi
Olfactory bulb	OB
Olfactory nerve layer	ON
1.1.2. CEREBRUM/CEREBRAL CORTEX	CER
Olfactory cortex	OlfC
Olfactry tubercle	Tu
Islands of Calleja	ICj
Islands of Calleja/major island	ICjM
Tenia tecta	TT
Cortical areas	CorA
Agranular insular cortex	AI
Anterior intraparietal area of the cortex	AIP
Areas 1 and 2 of the cortex	A1/2
Area 3a of the cortex (primary somatosensory)	A3a
Area 3b of the cortex (primary somatosensory)	A3b
Area 4 of the cortex/parts a and b (primary motor)	A4ab
Area 4 of the cortex/part c (primary motor)	A4c
Area 6 of the cortex/dorsocaudal part	A6DC
Area 6 of the cortex/dorsorostral part	A6DR
Area 6 of the cortex/medial (supplementary motor) part	A6M
Area 6 of the cortex/ventral/part a	A6Va
Area 6 of the cortex/ventral/part b	A6Vb
Area 8a of the cortex/dorsal part	A8aD
Area 8a of the cortex/ventral part	A8aV
Area 8b of the cortex	A8b
Area 8 of the cortex/caudal part	A8C
Area 9 of the cortex	A9
Area 10 of the cortex	A10
Area 11 of the cortex	A11
Area 13a of the cortex	A13a
Area 13b of the cortex	A13b
Area 13 of the cortex/lateral part	A13L
Area 13 of the cortex/medial part	A13M
Area 14 of the cortex/caudal part	A14C
Area 14 of the cortex/rostral part	A14R
Area 19 of the cortex/dorsointermediate part	A19DI
Area 19 of the cortex/medial part	A19M
Area 23a of the cortex	A23a
Area 23b of the cortex	A23b
Area 23c of the cortex	A23c
Area 23 of the cortex/ventral part	A23V
Area 24a of the cortex	A24a
Area 24b of the cortex	A24b
Area 24c of the cortex	A24c
Area 24d of the cortex	A24d
Area 25 of the cortex	A25
Area 29a–c of the cortex	A29a–c
Area 29d of the cortex	A29d
Area 30 of the cortex	A30
Area 31 of the cortex	A31
Area 32 of the cortex	A32
Area 32 of the cortex/ventral part	A32V
Area 35 of the cortex	A35
Area 36 of the cortex	A36
Area 45 of the cortex	A45
Area 46 of the cortex/dorsal part	A46D
Area 46 of the cortex/ventral part	A46V
Area 47 (old 12) of the cortex/lateral part	A47L
Area 47 (old 12) of the cortex/medial part	A47M
Area 47 (old 12) of the cortex/orbital part	A47O

1.1.2. CEREBRUM/CEREBRAL CORTEX (cont.)	CER
Auditory cortex/anterolateral area	AuAL
Auditory cortex/caudolateral area	AuCL
Auditory cortex/caudomedial area	AuCM
Auditory cortex/caudal parabelt area	AuCPB
Auditory cortex/middle lateral area	AuML
Auditory cortex/primary area	AuA1
Auditory cortex/rostral area	AuR
Auditory cortex/rostral parabelt	AuRPB
Auditory cortex/rostromedial area	AuRM
Auditory cortex/rostrotemporal lateral area	AuRTL
Auditory cortex/rostrotemporal medial area	AuRTM
Auditory cortex/rostrotemporal part	AuRT
Dysgranular insular cortex	DI
Entorhinal cortex	Ent
Faciola cinereum	FC
Fundus of the superior temporal sulcus area of the cortex	FST
Granular insular cortex	GI
Gustatory cortex	Gu
Indusium griseum	IG
Insular proisocortex	IPro
Lateral intrapartietal area of the cortex	LIP
Medial intraparietal area of the cortex	MIP
Medial superior temporal area of the cortex	MST
Navicular nucleus of the basal forebrain	Nv
Occipito-parietal transitional area of the cortex	OPt
Orbital periallocortex	OPAl
Orbital proisocortex	OPro
Parainsular cortex/lateral part	PaIL
Parainsular cortex/medial part	PaIM
Parasubiculum	PaS
Parietal area PE	PE
Parietal area PE/caudal part	PEC
Parietal area PF	PF
Parietal area PFG	PFG
Parietal area PG	PG
Parietal areas PGa and IPa (fundus of superior temporal ventral area)	PGa/IPa
Parietal area PG/medial part	PGM
Piriform cortex	Pir
Piriform cortex/layer 1	Pir 1
Piriform cortex/layer 2	Pir 2
Piriform cortex/layer 3	Pir 3
Presubiculum	PrS
Proisocortical motor region (precentral opercular cortex)	ProM
Prostriate area	ProSt
Prosubiculum	ProS
Retroinsular area	ReI
Secondary somatosensory cortex/external part	S2E
Secondary somatosensory cortex/internal part	S2I
Secondary somatosensory cortex/parietal rostral area	S2PR
Secondary somatosensory cortex/parietal ventral area	S2PV
Superior temporal rostral area	STR
Supracallosal subiculum	SS
Temporal area TE1	TE1
Temporal area TE2	TE2
Temporal area TE3	TE3
Temporal area TE/occipital part	TEO
Temporal area TF	TF
Temporal area TF/occipital part	TFO
Temporal area TH	TH
Temporal area TL	TL
Temporal area TL/occipital part	TLO
Temporal proisocortex	TPro
Temporo-parieto-occipital association area (superior temporal polysensory cortex)	TPO
Temporopolar proisocortex	TPPro
Temporoparietal transitional area	TPt
Ventral intraparietal area of the cortex	VIP
Visual area 1	V1
Visual area 2	V2
Visual area 3 (ventrolateral posterior area)	V3
Visual area 3A (dorsoanterior area)	V3A
Visual area 4 (ventrolatereral anterior area)	V4
Visual area 4/transitional part	V4T
Visual area 5 (middle temporal area)	V5
Visual area 6 (dorsomedial area)	V6
Visual area 6A (posterior parietal medial area)	V6A

Table 1 (*Continued*)

1.1.2. CEREBRUM/CEREBRAL CORTEX (cont.)	CER	
Hippocampal formation	HipF	
Dentate gyrus	DG	
Granule cell layer of the dentate gyrus	GrDG	
Molecular layer of the dentate gyrus	MoDG	
Polymorph layer of the dentate gyrus	PoDG	
Hippocampus	Hip	
Field CA1 of the hippocampus	CA1	
Field CA2 of the hippocampus	CA2	
Field CA3 of the hippocampus	CA3	
Lacunosum moleculare layer of the hippocampus	LMol	
Oriens layer of the hippocampus	Or	
Pyramidal cell layer of the hippocampus	Py	
Radiatum layer of the hippocampus	Rad	
Stratum lucidum of the hippocampus	SLu	
Subiculum	S	
1.1.3. BASAL GANGLIA	BG	
Amygdala	AMG	
Amygdalohippocampal area	AHi	
Amygdalopiriform transition area	APir	
Amygdalostriatal transition area	ASt	
Cortical amygdaloid group (corticomedial group)	CoAG	
Central amygdaloid nucleus	Ce	
Central amygdaloid nucleus/capsular parts	CeC	
Central amygdaloid nucleus/lateral parts	CeL	
Central amygdaloid nucleus/medial parts	CeM	
Cortical amugdaloid nucleus	Co	
Anterior amygdaloid area	AA	
Anterior cortical amygdaloid nucleus	ACo	
Nucleus of the lateral olfactry tract	LOT	
Posterior cortical amygdaloid nucleus	PCo	
Medial amygdaloid nucleus	Me	
Cortex-amygdala transition zone	CxA	
Extended amygdala	EXA	
Extended amygdala	EA	
Bed nucleus of the stria terminalis	ST	
Bed nucleus of the stria terminalis/fusiform part	Fu	
Bed nucleus of the stria terminalis/intraamygdaloid division	STIA	
Bed nucleus of the stria terminalis/lateral division; dorsal part	STLD	
Bed nucleus of the stria terminalis/lateral division; posterior part	STLP	
Bed nucleus of the stria terminalis/medial division; anterior part	STMA	
Bed nucleus of the stria terminalis/medial division; posterior part	STMP	
Bed nucleus of the stria terminalis/medial division; ventral part	STMV	
Intercalated nuclei of the amygdala	I	
Intercalated amygdaloid nucleus; main part	IM	
Interstitial nucleus of the posterior limb of the anterior commissure	IPAC	
Latero-basal nuclear complex (bassolateral group)	Lbn	
Basolateral amygdaloid nucleus	BL	
Basolateral amygdaloid nucleus/dorsal part	BLD	
Basolateral amygdaloid nucleus/dorsolateral part	BLDL	
Basolateral amygdaloid nucleus/intermediate part	BLI	
Basolateral amygdaloid nucleus/ventrolateral part	BLVL	
Basolateral amygdaloid nucleus/ventromedial part	BLVM	
Basomedial amygdaloid nucleus	BM	
Basomedial amygdaloid nucleus/dorsal part	BMD	
Basomedial amygdaloid nucleus/magnocellular part	BMMC	
Basomedial amygdaloid nucleus/parvicellular part	BMPC	
Basomedial amygdaloid nucleus/ventral part	BMV	
Basomedial amygdaloid nucleus/vebtromedial part	BMVM	
Lateral amygdaloid nucleus	La	
Paralaminar amygdaloid nucleus	PaL	

1.1.3. BASAL GANGLIA (cont.)	BG	
Basal nucleus (Meynert)	B	
Claustrum	Cl	
Dorsal nucleus of the endopiriform claustrum	DEn	
Globus pallidus	GP	
External globus pallidus	EGP	
Internal globus pallidus	IGP	
Intermediate endopiriform nucleus	IEn	
Substania innominata; basal part	SIB	
Substantia nigra	SNBG	
Substantia nigra; compact part	SNC	
Substantia nigra; compact part/dorsal tier	SNCD	
Substantia nigra; compact part/medial tier	SNCM	
Substantia nigra; compact part/ventral tier	SNCV	
Substantia nigra; lateral part	SNL	
Substantia nigra; reticular part	SNR	
Striatum	St	
Accumbens nucleus	Acb	
Accumbens nucleus; core	AcbC	
Accumbens nucleus;shell	AcbSh	
Dorsal accumbens shell	DAcbSh	
Lateral accumbens shell	LAcbSh	
Medial accumbens shell	MAcbSh	
Caudate nucleus	Cd	
Putamen	Pu	
Subthalamic nucleus	STh	
Ventral nucleus of the endopiriform claustrum	VEn	
Ventral pallidum	VP	
1.1.4. SEPTUM	SEP	
Nucleus of the horizontal limb of the diagonal band	HDB	
Nucleus of the vertical limb of the diagonal band	VDB	
Lambdoid spetal zone	Ld	
Lateral nucleus of the diagonal band	LDB	
Lateral septal nuclei	LS	
Lateral septal nucleus;dorsal part	LSD	
Lateral septal nucleus; intermediate part	LSI	
Lateral septal nucleus; ventral part	LSV	
Medial septal nucleus	MS	
Paradiagonal zone	PDZ	
Septofimbrial nucleus	SFi	
Septohippocampal nucleus	SHi	
Triangular septal nucleus	TS	
1.2. DIENCEPHALON	DIEN	
1.2.1. THALAMUS	THAL	
Association nuclei	ASN	
Anterior nuclei	ANN	
Anterodorsal thalamic nucleus	AD	
Anteromedial thalamic nucleus	AM	
Anteroventral thalamic nucleus	AV	
Lateral nuclei	LTN	
Lateral posterior thalamic nucleus	LP	
Laterodorsal thalamic nucleus	LD	
Mediodorsal thalamic nucleus	MD	
Mediodorsal thalamic nucleus/central part	MDC	
Mediodorsal thalamic nucleus/lateral part	MDL	
Mediodorsal thalamic nucleus/medial part	MDM	
Paratenial nucleus	PT	
Pulvinar	Pul	
Anterior pulvinar	APul	
Inferior pulvinar	IPul	
Inferior pulvinar/caudolateral part	IPulCL	
Inferior pulvinar/caudomedial part	IPulCM	
Inferior pulvinar/medial part	IPulM	
Inferior pulvinar/posterior part	IPulP	
Lateral pulvinar	LPul	
Medial pulvinar	MPul	

Table 1 (*Continued*)

1.2.1. THALAMUS (cont.)	THAL	
Auditory thalamus	AuT	
Medial geniculate nucleus	MG	
Medial geniculate nucleus/dorsal part	MGD	
Medial geniculate nucleus/medial part	MGM	
Medial geniculate nucleus/ventral part	MGV	
Midline and intralaminar nuclei	MIN	
Angular thalamic nucleus	Ang	
Central medial thalamic nucleus	CM	
Centrolateral thalamic nucleus	CL	
Centromedian thalamic nucleus	CMn	
Interanteromedial thalamic nucleus	IAM	
Intermediodorsal thalamic nucleus	IMD	
Oval paracentral thalamic nucleus	OPC	
Paracentral thalamic nucleus	PC	
Parafascicular thalamic nucleus	PaF	
Posterior intralaminar thalamic nucleus	PIL	
Posterior limitans thalamic nucleus	PLi	
Retroreuniens nucleus	RRe	
Reuniens thalamic nucleus	Re	
Rhomboid thalamic nucleus	Rh	
Xiphoid thalamic nucleus	Xi	
Motor thalamus	MTT	
Ventral anterior thalamic nucleus	VA	
Ventral anterior thalamic nucleus/lateral part	VAL	
Ventral anterior thalamic nucleus/magnocellular part	VAMC	
Ventral anterior thalamic nucleus/medial part	VAM	
Ventral lateral thalamic nucleus	VL	
Ventral lateral thalamic nucleus/lateral part	VLLa	
Ventral lateral thalamic nucleus/medial part	VLM	
Ventrolateral thalamic nucleus/dorsal part	VLD	
Ventrolateral thalamic nucleus/ventral part	VLV	
Somatosensory thalamus	SST	
Ethmoid thalamic nucleus	Eth	
Posterior thalamic nuclear group	Po	
Posterior thalamic nuclear group/triangular part	PoT	
Suprageniculate thalamic nucleus	SG	
Ventral posterior thalamic nucleus/inferior part	VPI	
Ventral posterior thalamic nucleus/superior part	VPS	
Ventoposterior complex	VPC	
Ventral posterior nucleus of the thalamus/parvicellular	VPPC	
Ventral posterolateral thalamic nucleus	VPL	
Ventral posteromedial thalamic nucleus	VPM	
Ventral thalamus	VNT	
Parasubthalamic nucleus	PSTh	
Reticular nucleus	Rt	
Subgeniculate nucleus of prethalamus	SubG	
Subincertal nucleus	SubI	
Subparafiscicular thalamic nucleus	SPF	
Subparafiscicular thalamic nucleus/parvicellular part	SPFPC	
Zona incerta	ZI	
Zona incerta/caudal part	ZIC	
Zona incerta/dorsal part	ZID	
Zona incerta/rostral part	ZIR	
Zona incerta/ventral part	ZIV	
Visual thalamus	VST	
Dorsal lateral geniculate nucleus	DLG	
External magnocellular layer of the dorsal lateral geniculate	ExMC	
External parvicellular layer of the dorsal lateral geniculate	ExPC	
Internal magnocellular layer of the dorsal lateral geniculate	InMC	
Internal parvicellular layer of the dorsal lateral geniculate	InPC	
Koniocellular layer of the dorsal latral geniculate K1	K1	
Koniocellular layer of the dorsal latral geniculate K2	K2	
Koniocellular layer of the dorsal latral geniculate K3	K3	
Koniocellular layer of the dorsal latral geniculate K4	K4	
Pregeniculate nucleus	PrG	

1.2.2. EPITHALAMUS	EPI	
Habenular nucleus	Hb	
Lateral habenular nucleus	LHb	
Medial habenular nucleus	MHb	
Paraventricular thalamic nucleus	PV	
Paraventricular thalamic nucleus/anterior part	PVA	
Paraventricular thalamic nucleus/posterior part	PVP	
1.2.3. HYPOTHALAMUS	HYPO	
Anterior hypothalamic area/anterior part	AHA	
Anterior hypothalamic nucleus	AH	
Anteroventral periventricular nucleus	AVPe	
Arcuate hypothalamic nucleus	Arc	
DA11 dopamine cells	DA11	
DA12 dopamine cells	DA12	
DA14 dopamine cells	DA14	
Dorsomedial hypothalamic nucleus	DM	
Dorsomedial hypothalamic nucleus/compact part	DMC	
Juxtaparaventricular part of the lateral hypothalamus	JPLH	
Lamina terminalis	Lter	
Lateral hypothalamic area	LH	
Mammillary body	MB	
Lateral mammillary nucleus	LM	
Medial mammillary nucleus/lateral part	ML	
Medial mammillary nucleus/medial part	MM	
Medial tuberal nucleus	MTu	
Nucleus of the stria medullaris	SM	
Paraventricular hypothalamic nucleus	Pa	
Paraventricular hypothalamic nucleus/dorsal cap	PaDC	
Paraventricular hypothalamic nucleus/lateral magnocellular part	PaLM	
Paraventricular hypothalamic nucleus/posterior part	PaPo	
Perifornical nucleus	PeF	
Periventricular hypothalamic nucleus	Pe	
Posterior hypothalamic nucleus	PH	
Premammillary nucleus/dorsal part	PMD	
Premammillary nucleus/ventral part	PMV	
Preoptic area	PO	
Lateral preoptic area	LPO	
Medial preoptic area	MPA	
Medial preoptic nucleus	MPO	
Median preoptic nucleus	MnPO	
Retromammillary nucleus	RM	
Striohypothalamic nucleus	StHy	
Suprachiasmatic nucleus	SCh	
Supraoptic nucleus	SO	
Supraoptic nucleus/retrochiasmatic part	SOR	
Ventral tuberomammillary nucleus	VTM	
Ventrolateral preoptic nucleus	VLPO	
Ventromedial hypothalamic nucleus	VMH	
Ventromedial preoptic nucleus	VMPO	
1.2.4. PRETECTUM	Pt	
Anterior pretectal nucleus	APT	
Magnocellular nucleus of the posterior commissure	MCPC	
Medial pretectal area	MPT	
Nucleus of the optic tract	OT	
Olivary pretectal nucleus	OPT	
Precommissural nucleus	PrC	
Retrocommissural nucleus	ReC	

Table 1 (*Continued*)

2. BRAIN STEM (MIDBRAIN+PONS+MEDULLA OBLONGATA)	STEM
2.1. MIDBRAIN (MESENCEPHALON)	MID
Commissural nucleus of the inferior colliculus	Com
DA8 dopamine cells	DA8
Edinger–Westphal nucleus	EW
Interoculomotor nucleus	I3
Inferior colliculus	IC
Central nucleus of the inferior colliculus	CIC
Dorsal cortex of the inferior colliculus	DCIC
External cortex of the inferior colliculus	ECIC
Interstitial nucleus of Cajal	InC
Interpeduncular nucleus	IP
Interpeduncular nucleus/apical subnucleus	IPA
Interpeduncular nucleus/caudal subnucleus	IPC
Interpeduncular nucleus/intermediate subnucleus	IPI
Interpeduncular nucleus/lateral subnucleus	IPL
Interpeduncular nucleus/rostral subnucleus	IPR
Medial accessory oculomotor nucleus	MA3
Mesencephalic trigeminal nucleus	Me5
Nucleus of the brachium of the inferior colliculus	BIC
Nucleus of Darkschewitsch	Dk
Nucleus of the posterior commissure	PCom
Occulomotor nucleus	3N
Occulomotor nucleus/parvicellular part	3PC
Periaqueductal gray	PAG
Dorsolateral periaqueductal gray	DLPAG
Dorsomedial periaqueductal gray	DMPAG
Lateral periaqueductal gray	LPAG
Pleioglia periaqueductal gray	PlPAG
Supraoculomotor cap	Su3C
Supraoculomotor periaqueductal gray	Su3
Ventrolateral periaqueductal gray	VLPAG
Parabrachial pigmented nucleus of the VTA	PBP
Parainterfascicular nucleus of the ventral tegmental area	PIF
Paranigral nucleus of the VTA	PN
Peripeduncular nucleus	PP
Prerubral field	PR
Red nucleus	R
Red nucleus/magnocellular part	RMC
Red nucleus/parvicellular part	RPC
Raphe nuclei	RaMID
Dorsal raphe nucleus	DR
Dorsal raphe nucleus/caudal part	DRC
Dorsal raphe nucleus/dorsal part	DRD
Dorsal raphe nucleus/interfascicular part	DRI
Dorsal raphe nucleus/lateral part	DRL
Dorsal raphe nucleus/ventral part	DRV
Dorsal raphe nucleus/ventrolateral part	DRVL
Rostral linear nucleus	RLi
Reticular formation	RtMID
Cuneinform nucleus	CnF
Mesencephlic reticular formation	mRt
Precuneiform area	PrCnF
Rostral interstitial nucleus of the medial longitudinal fasciculus	RI
Superior colliculus	SC
Deep gray layer of the superior colliculus	DpG
Deep white layer of the superior colliculus	DpWh
Intermediate gray layer of the superior colliculus	InG
Intermediate white layer of the superior colliculus	InWh
Optic nerve layer of the superior colliculus	Op
Superficial gray layer of the superior colliculcus	SuG
Zonal layer of the superior colliculus	Zo
Subbrachial nucleus	SubB
Substantia nigra	SNMID
Trochlear nucleus	4N
Ventral tegmental area	VTA
Ventral tegmental area/caudal part	VTAC
Ventral tegmental area/rostral part	VTAR
2.2. PONS (METENCEPHALON)	PONS
Abducens nucleus	6N
Anterior tegmental nucleus	ATg
B9 serotonin cells	B9
Barrington's nucleus	Bar
Central gray	CG
Cochlear nuclei	C
Dorsal cochlear nucleus	DC
Granule cell layer of the cochlear nuclei	GrC
Ventral cochlear nucleus/anterior part	VCA
Ventral cochlear nucleus/posterior part	VCP

2.2. PONS (METENCEPHALON) (cont.)	PONS
Dorsal nucleus of the lateral lemniscus	DLL
Dorsal tegmental nucleus	DTg
Facial nucleus	7N
Facial motor nucleus; stylohyoid part	7SH
Intermediate nucleus of the lateral lemniscus	ILL
Locus coeruleus	LC
Laterodorsal tegmental nucleus	LDTg
Laterodorsal tegmental nucleus; ventral part	LDTgV
Parabrachial nuclei	PB
Lateral parabrachial nucleus	LPB
Lateral parabrachial nucleus/central part	LPBC
Lateral parabrachial nucleus/crescent part	LPBCr
Lateral parabrachial nucleus/dorsal part	LPBD
Lateral parabrachial nucleus/external part	LPBE
Lateral parabrachial nucleus/internal part	LPBI
Lateral parabrachial nucleus/superior part	LPBS
Lateral parabrachial nucleus/ventral part	LPBV
Medial parabrachial nucleus	MPB
Medial parabrachial nucleus/external part	MPBE
Medial paralemniscial nucleus	MPL
Microcellular tegmental nucleus	MiTg
Motor trigeminal nucleus	5N
Motor trigeminal nucleus/parvicellular part	5PC
NA5 noradrenalin cells	NA5
NA7 noradrenalin cells	NA7
Nucleus of the central acoustic tract	CAT
Nucleus of the spinal trigeminal tract	Sp5PONS
Nucleus of the trapezoid body	Tz
Parabigeminal nucleus	PBG
Paralemniscal nucleus	PL
Pedunculotegmental nucleus	PTg
Peritrigeminal zone	P5
Pontine nuclei	Pn
Posterodorsal tegmental nucleus	PDTg
Principal sensory trigeminal nucleus	Pr5
Principal sensory trigeminal nucleus/dorsomedial part	Pr5DM
Principal sensory trigeminal nucleus/ventrolateral part	Pr5VL
Raphe nuclei	RaPONS
Caudal linear nucleus of the raphe	CLi
Dorsal raphe nucleus/caudal part	DRC
Median raphe nucleus	MnR
Paramedian raphe nucleus	PMnR
Raphe interpositus nucleus	RIP
Raphe magnus nucleus	RMg
Rhabdoid nucleus	Rbd
Reticular formation	RtPONS
Pontine reticular nucleus/caudal part	PnC
Pontine reticular nucleus/oral part	PnO
Pontine reticular nucleus/ventral part	PnV
Reticulotegmental nucleus of the pons	RtTg
Reticulotegmental nucleus of the pons/lateral part	RtTgL
Retroisthmic nucleus	RIs
Retrolemniscal nucleus	RL
Sagulum nucleus	Sag
Subcoeruleus nucleus/dorsal part	SubCD
Subcoeruleus nucleus/ventral part	SubCV
Subpeduncular tegmental nucleus	SPTg
Superior olive	SOI
Dorsal periolivary region	DPO
Lateral superior olive	LSO
Laterоventral periolivary nucleus	LVPO
Medial superior olive	MSO
Medioventral periolivary nucleus	MVPO
Superior paraolivary nucleus	SPO
Supratrigeminal nucleus	Su5
Triangular nucleus of the lateral lemniscus	TrLL
Ventral nucleus of the lateral lemniscus	VLL
Vestibular nuclei	VePONS

Table 1 (*Continued*)

2.3. MEDULLA OBLONGATA (MYELENCEPHALON)	MED
Accessory nerve nucleus	11N
Ad1 adrenalin cells	Ad1
Ambiguus nucleus	Amb
Ambiguus nucleus/compact part	AmbC
Ambiguus nucleus/loose part	AmbL
Botzinger complex	Bo
Conterminal nucleus	Ct
Cuneate nucleus	Cu
Dorsal motor nucleus of the vagus/caudal part	10Ca
Epifacicular nucleus	EF
External cuneate nucleus	ECu
Gracile nucleus	Gr
Hypoglossal nucleus	12N
Hypoglossal nucleus/geniohyyoid part	12GH
Inferior olive	IO
Inferior olive/beta subnucleus of the medial nucleus	IOBe
Inferior olive/cap of Kooy of the medial nucleus	IOK
Inferior olive/dorsal nucleus	IOD
Inferior olive/medial nucleus	IOM
Inferior olive/principal nucleus	IOPr
Inferior olive/subnucleus A of the medial nucleus	IOA
Inferior olive/subnucleus B of the medial nucleus	IOB
Inferior olive/subnucleus C of the medial nucleus	IOC
Inferior salivatory nucleus	IS
Intercalated nucleus	In
Interstitial nucleus of the vestibular part of the 8th nerve	I8
Koelliker-Fuse nucleus	KF
Lateral pericuneate nucleus	LPCu
Lateral terminal nucleus of the accessory optic tract	LT
Linear nucleus of the hindbrain	Li
Matrix region of the medulla	Mx
Median accessory nucleus of the medulla	MnA
NA1 noradrenalin cells	NA1
NA2 noradrenalin cells	NA2
Noto cuneate nucleus	Nt
Nucleus of Roller	Ro
Nucleus of the spinal trigeminal tract	Sp5MED
Spinal trigeminal nucleus/caudal part	Sp5C
Spinal trigeminal nucleus/interpolar part	Sp5I
Spinal trigeminal nucleus/oral part	Sp5O
Nucleus X	X
Parasolitary nucleus	PSol
Paratrigeminal nucleus	Pa5
Prepositus nucleus	Pr
Prepositus nucleus/magnocellular part	PrMC
Raphe nuclei	RaMED
Raphe obscurus nucleus	ROb
Raphe pallidus nucleus	RPa
Reticular formation	RtMED
Caudoventrolateral reticular nucleus	CVL
Dorsal paragigantocellular nucleus	DPGi
Gigantocellular reticular nucleus	Gi
Gigantocellular reticular nucleus/alpha part	GiA
Gigantocellular reticular nucleus/ventral part	GiV
Intermediate reticular nucleus	IRt
Lateral paragigantocellular nucleus	LPGi
Lateral reticular nucleus	LRt
Lateral reticular nucleus/parvicellular part	LRtPC
Lateral reticular nucleus/subtrigeminal part	LRtS5
Medullary reticular nucleus/dorsal part	MdD
Medullary reticular nucleus/ventral part	MdV
Parvicellular reticular nucleus	PCRt
Parvicellular reticular nucleus/alpha part	PCRtA
Rostroventrolateral reticular nucleus	RVL
Retroambiguus nucleus	RAmb
Rostral ventral respiratory group	RVRG

2.3. MEDULLA OBLONGATA (MYELENCEPHALON) (cont.)	MED
Solitary nucleus	Sol
Solitary nucleus/commissural part	SolC
Solitary nucleus/dorsolateral part	SolDL
Solitary nucleus/gelatinous part	SolG
Solitary nucleus/intermediate part	SolIM
Solitary nucleus/interstitial part	SolI
Solitary nucleus/medial part	SolM
Solitary nucleus/paracommissural part	SolPaC
Solitary nucleus/rostrolateral part	SolRL
Solitary nucleus/ventral part	SolV
Solitary nucleus/ventrolateral part	SolVL
Superior salivatory nucleus	SuS
Vestibular nuclei	VeMED
Lateral vestibular nucleus	LVe
Medial vestibular nucleus	MVe
Medial vestibular nucleus/magnocellular part	MVeMC
Medial vestibular nucleus/parvicellular part	MVePC
Nucleus Y of the vestibular complex	Y
Spinal vestibular nucleus	SpVe
Superior vestibular nucleus	SuVe
Vagus nerve nucleus	10N
3. CEREBELLUM (METENCEPHALON)	CB
Cerebellar cortex	Cb
Copula of the pyramis	Cop
Crus1 of the ansiform lobule	Crus1
Crus2 of the ansiform lobule	Crus2
Flocculus	Fl
Lobule 1 of the cerebellar vermis (lingula)	1Cb
Lobule 2 of the cerebellar vermis	2Cb
Lobule 3 of the cerebellar vermis	3Cb
Lobule 4 of the cerebellar vermis	4Cb
Lobule 5 of the cerebellar vermis	5Cb
Lobule 6 of the cerebellar vermis	6Cb
Lobule 7 of the cerebellar vermis	7Cb
Lobule 8 of the cerebellar vermis	8Cb
Lobule 9 of the cerebellar vermis (uvula)	9Cb
Lobule 10 of the cerebellar vermis (nodule)	10Cb
Paraflocculus	PFl
Paramedian lobule	PM
Simple lobule	Sim
Deep cerebellar nuclei	Dc
Anterior interposed cerebellar nucleus	IntA
Lateral (dentate) cerebellar nucleus	Lat
Lateral cerebellar nucleus/parvicellular part	LatPC
Medial cerebellar nucleus	Med
Posterior interposed cerebellar nucleus	IntP
Vestibulocerebellar nucleus	VeCb
Superior medullary velum	SMV
4. FIBER BUNDLE	FB
Ansa lenticularis	al
Alveus of the hippocampus	alv
Anterior commissure	ac
Anterior commissure/anterior part	aca
Anterior commissure/intrabulbar part	aci
Anterior commissure/posterior limb	acp
Ascending fibers of the facial nerve	asc7
Brachium of the inferior colliculus	bic
Brachium of the superior colliculus	bsc
Cerebral peduncle	cp
Cingulum	cg
Corpus callosum	cc
Commissural stria terminals	cst
Commissure of the inferior colliculus	cic
Commissure of the lateral leminiscus	cll
Commissure of the superior colliculus	csc
Cuneate fasciculus	cu
Decussation of the medial lemniscus	xml
Decussation of the superior cerebellar peduncle	xscp
Dorsal acoustic atria	das
Dorsal corticospinal tract	dcs
Dorsal spinocerebellar tract	dsc
Dorsal tegmental decussation	dtgx

Table 1 (*Continued*)

4. FIBER BUNDLE (cont.)	FB
External capsule	ec
External medullary lamina	eml
Extreme capsule	ex
Fasciculus retroflexus	fr
Fimbria of the hippocampus	fi
Forceps minor corpus callosum	fmi
Fornix	f
Genu of the corpus callosum	gcc
Genu of the facial nerve	g7
Gracile fasciculus	gr
h1 fasciculus (thalamic fasciculus)	h1
h2 fasciculus (lenticular fasciculus)	h2
Habenular commissure	hbc
Inferior cerebellar peduncle	icp
Internal capsule	ic
Lateral corticospinal tract	lcs
Lateral lemniscus	ll
Lateral medullary lamina	lml
Lateral olfactory tract	lo
Longitudinal fasciculs of the pons	lfp
Mammillary peduncle	mp
Mammillotegmental tract	mtg
Mammillothalamic tract	mt
Medial forebrain bundle	mfb
Medial lemniscus	ml
Medial longitudinal faciculcus	mlf
Medial medullar lamina	mml
Mesencephalic trigeminal tract	me5
Middle cerebellar peduncle	mcp
Motor root of the trigeminal nerve	m5
Nigrostriatal bundle	ns
Olivocerebellar tract	oc
Olivocochlear bundle	ocb
Optic chiasm	och
Optic tract	opt
Palidohypothalamic tract	palhy
Posterior commissure	pc
Pyramidal tract	py
Pyramidal decussation	pyx
Retromammillary decussation	rmx
Rostrum of the corpus callosum	rcc
Rubrospinal tract	rs
Sensory root of the trigeminal nerve	s5
Solitary tract	sol
Spinal trigeminal tract	sp5
Stria medullaris of the thalamus	sm
Stria terminalis	st
Supraoptic decussation	sox
Superior cerebellar peduncle	scp
Tectospinal tract	ts
Transverse fibers of the pons	tfp
Trapezoid body	tz
Ventral hippocampal commissure	vhc
Ventral spinocerebellar tract	vsc
Ventral tegmental decussation	vtgx
Vestibulomesencephalic tract	veme

5. CRANIAL NERVE	CN
Abducens nerve	6n
Cochlear root of the vestibulocochlear nerve	8cn
Facial nerve	7n
Hypoglossal nerve	12n
Nervus intermedius component of facial nerve	7ni
Occulomotor nerve	3n
Optic nerve	2n
Trigeminal nerve	5n
Trochlear nerve	4n
Vestibular root of the vestibulocochlear nerve	8vn
Vestibulocochlear nerve	8n
6. CIRCUMVENTRICULAR ORGAN	CvO
Area postrema	AP
Median eminence	ME
Neurohypophysis	Nhyp
Pineal gland	Pi
Subcommissural organ	SCO
Subfornical organ	SFO
Vascular organ of the lamina terminalis	VOLT
7. VENTRICLE	V
Aqueduct	Aq
Central canal	CC
Dorsal 3rd ventricle	D3V
Fourth ventricle	4V
Interventricular foramen	IVF
Lateral recess of the 4th ventricle	LR4V
Lateral ventricle	LV
Mammillary recess of the 3rd ventricle	Mre
Recess of the inferior colliculus	ReIC
Third ventricle	3V
8. SULCUS	SUL
Calcarine sulcus	cal
Hippocampal fissure	hif
Intraparietal sulcus	ips
Lateral fissure	lf
Occipitotemporal sulcus	ots
Orbital sulcus	orbs
Posterolateral fissure	plf
Preculminate fissure	pcuf
Prepyramidal fissure	ppf
Primary fissure	prf
Rhinal fissure	rf
Secondary fissure	sf
Superior temporal sulcus	sts
Ventromedian fissure	vmf

planes with the horizontal axis passing through the bicommissural line could also be reproduced using the model (Fig. 7). The model can also produce serial 2D images from virtual sections reconstructed from the 3D model to facilitate the comparison of the histological sections with radiological sections at the same levels.

6. Conclusion

In this article, several kinds of brain atlases for the common marmoset monkey (*Callithrix jacchus*) were reviewed. These atlases include: a histological atlas with stereotaxic coordinates, an atlas that combined histological information with MRI data in stereotaxic coordinates, and an axial-free 3D volume-rendered model reconstructed from histological sections. Of the reviewed atlas types, we propose that a volume-rendered model will pose most useful for studies done on the common marmoset.

Acknowledgments

This study was supported by grants FIRST and Brain/MINDS from MEXT Japan.

References

Ash, H., Buchanan-Smith, H.M., 2014. Long-term data on reproductive output and longevity in captive female common marmosets (*Callithrix jacchus*). Am. J. Primatol. 76, 1062–1073.

Berman, A.L., 1968. The Brain Stem of the Cat: A Cytoarchitectonic Atlas With Stereotaxic Coordinates. University of Wisconsin Press, Madison, WI, 175 pp.

Berman, A.L., Jones, E.G., 1982. The Thalamus and Basal Telencephalon of the Cat: A Cytoarchitectonic Atlas With Stereotaxic Coordinates. University of Wisconsin Press, Madison, WI, 164 pp.

Carson, J.P., Ju, T., Lu, H.C., Thaller, C., Xu, M., Pallas, S.L., Crair, M.C., Warren, J., Chiu, W., Eichele, G., 2005. A digital atlas to characterize the mouse brain transcriptome. PLoS Comput. Biol. 1, e41.

Dorr, A.E., Lerch, J.P., Spring, S., Kabani, N., Henkelman, R.M., 2008. High resolution three-dimensional brain atlas using an average magnetic resonance image of 40 adult C57Bl/6J mice. Neuroimage 42, 60–69.

Hardman, C.D., Ashwell, K.W.S., 2012. Stereotaxic and Chemoarchitectural Atlas of the Brain of the Common Marmoset (*Callithrix jacchus*). CRC Press, Boca Raton, FL, 506 pp.

Hawrylycz, M., Baldock, R.A., Burger, A., Hashikawa, T., Johnson, G.A., Martone, M., Ng, L., Lau, C., Larson, S.D., Larsen, S.D., et al., 2011. Digital atlasing and standardization in the mouse brain. PLoS Comput. Biol. 7, e1001065.

Heig, D., 1999. What is a marmoset? Am. J. Primatol. 49, 285–296.

Hevner, R.F., 2007. Layer-specific markers as probes for neuron type identity in human neocortex and malformations of cortical development. J. Neuropathol. Exp. Neurol. 66, 101–109.

Hikishima, K., Quallo, M.M., Komaki, Y., Yamada, M., Kawai, K., Momoshima, S., Okano, H.J., Sasaki, E., Tamaoki, N., Lemon, R.N., et al., 2011. Population-averaged standard template brain atlas for the common marmoset (*Callithrix jacchus*). Neuroimage 54, 2741–2749.

Hikishima, K., Sawada, K., Murayama, A.Y., Komaki, Y., Kawai, K., Sato, N., Inoue, T., Itoh, T., Momoshima, S., Iriki, A., et al., 2013. Atlas of the developing brain of the marmoset monkey constructed using magnetic resonance histology. Neuroscience 230, 102–113.

Hjornevik, T., Leergaard, T.B., Darine, D., Moldestad, O., Dale, A.M., Willoch, F., Bjaalie, J.G., 2007. Three-dimensional atlas system for mouse and rat brain imaging data. Front. Neuroinform. 1, 4.

Iriki, A., Okano, H.J., Sasaki, E., Okano, H. (Eds.), The 3D Stereotaxic Brain Atlas of the Common Marmoset (*Callothrix jacchus*). Springer, Tokyo, in press.

Jessberger, S., Gage, F.H., 2007. ZOOMING IN: a new high-resolution gene expression atlas of the brain. Mol. Syst. Biol. 3, 75.

Kishi, N., Sato, K., Sasaki, E., Okano, H., 2014. Common marmoset as a new model animal for neuroscience research and genome editing technology. Dev. Growth Differ. 56, 53–62.

Kumazawa-Manita, N., Katayama, M., Hashikawa, T., Iriki, A., 2013. Three-dimensional reconstruction of brain structures of the rodent *Octodon degus*: a brain atlas constructed by combining histological and magnetic resonance images. Exp. Brain Res. 231, 65–74.

Lein, E.S., Hawrylycz, M.J., Ao, N., Ayres, M., Bensinger, A., Bernard, A., Boe, A.F., Boguski, M.S., Brockway, K.S., Byrnes, E.J., et al., 2007. Genome-wide atlas of gene expression in the adult mouse brain. Nature 445, 168–176.

Ma, Y., Hof, P.R., Grant, S.C., Blackband, S.J., Bennett, R., Slatest, L., McGuigan, M.D., Benveniste, H., 2005. A three-dimensional digital atlas database of the adult C57BL/6J mouse brain by magnetic resonance microscopy. Neuroscience 135, 1203–1215.

Mano, M.T., Potter, B.J., Belling, G.B., Chavadej, J., Hetzel, B.S., 1987. Fetal brain development in response to iodine deficiency in a primate model (*Callithrix jacchus jacchus*). J. Neurol. Sci. 79, 287–300.

Marmoset Genome Sequencing and Analysis Consortium, 2014. The common marmoset genome provides insight into primate biology and evolution. Nat. Genet. 46, 850–857.

Martin, R.F., Bowden, D.M., 1996. A stereotaxic template atlas of the macaque brain for digital imaging and quantitative neuroanatomy. Neuroimage 4, 119–150.

Molyneaux, B.J., Arlotta, P., Menezes, J.R.L., Macklis, J.D., 2007. Neuronal subtypes specification in the cerebral cortex. Nat. Rev. Neurosci. 8, 427–437.

Newman, J.D., Kenkel, W.M., Aronoff, E.C., Bock, N.A., Zametkin, M.R., Silva, A.C., 2009. A combined histological and MRI brain atlas of the common marmoset monkey, *Callithrix jacchus*. Brain Res. Rev. 62, 1–18.

Ng, L., Bernard, A., Lau, C., Overly, C.C., Dong, H.W., Kuan, C., Pathak, S., Sunkin, S.M., Dang, C., Bohland, J.W., et al., 2009. An anatomic gene expression atlas of the adult mouse brain. Nat. Neurosci. 12, 356–362.

Norscia, I., Palagi, E., 2011. When play is a family business: adult play, hierarchy, and possible stress reduction in common marmosets. Primates 52, 101–104.

Palazzi, X., Bordier, N., 2008. The Marmoset Brain in Stereotaxic Coordinates. Springer, New York, NY, 64 pp.

Paxinos, G., Watson, C., Petrides, M., Rosa, M., Tokuno, H., 2012. The Marmoset Brain in Stereotaxic Coordinates. Academic Press/Elsevier.

Power, R.A., Power, M.L., Layne, D.G., Jaquish, C.E., Oftedal, O.T., Tardif, S.D., 2001. Relations among measures of body composition, age, and sex in the common marmoset monkey (*Callithrix jacchus*). Comp. Med. 51, 218–223.

Saleem, K., Logothetis, N., 2012. A Combined MRI and Histology: Atlas of the Rhesus Monkey Brain in Stereotaxic Coordinates. Academic Press/Elsevier.

Sasaki, E., Hanazawa, K., Kurita, R., Akatsuka, A., Yoshizaki, T., Ishii, H., Tanioka, Y., Ohnishi, Y., Suemizu, H., Sugawara, A., et al., 2005. Establishment of novel embryonic stem cell lines derived from the common marmoset (*Callithrix jacchus*). Stem Cells 23, 1304–1313.

Sasaki, T., Aoi, H., Oga, T., Fujita, I., Ichinohe, N., 2014. Postnatal development of dendritic structure of layer III pyramidal neurons in the medial prefrontal cortex of marmoset. Brain Struct. Funct., http://dx.doi.org/10.1007/s00429-014-0853-2.

Sawada, K., Hikishima, K., Murayama, A.Y., Okano, H.J., Sasaki, E., Okano, H., 2014. Fetal sulcation and gyrification in common marmosets (*Callithrix jacchus*) obtained by ex vivo magnetic resonance imaging. Neuroscience 257, 158–174.

Stephan, H., Baron, G., Schwerdtfeger, W.K., 2009. The Brain of the Common Marmoset (*Callithrix jacchus*). A Stereotaxic Atlas. Springer-Verlag, Berlin.

Stevenson, M.F., 1976. Birth and perinatal behaviour in family groups of the common marmoset (*Callithrix jacchus jacchus*), compared to other primates. J. Hum. Evol. 5, 365–381.

Tokuno, H., Tanaka, I., Umitsu, Y., Akazawa, T., Nakamura, Y., 2009. Web-accessible digital brain atlas of the common marmoset (*Callithrix jacchus*). Neurosci. Res. 64, 128–131.

Yuasa, S., Nakamura, K., Kohsaka, S., 2010. Stereotaxic Atlas of the Marmoset Brain with Immunohistochemical Architecture and MR Images. National Institute of Neuroscience, Tokyo.